Germinal center B cells govern their own fate via antibody feedback

Zhang, Yang; Meyer-Hermann, Michael; George, Laura A; Figge, Marc Thilo; Khan, Mahmood; Goodall, Margaret; Young, Stephen P; Reynolds, Adam; Falciani, Francesco; Waisman, Ari; Notley, Clare A; Ehrenstein, Michael R; Kosco-Vilbois, Marie; Toellner, Kai-Michael

DOI:
10.1084/jem.20120150

Document Version
Publisher's PDF, also known as Version of record

Citation for published version (Harvard):
Zhang, Y, Meyer-Hermann, M, George, LA, Figge, MT, Khan, M, Goodall, M, Young, SP, Reynolds, A, Falciani, F, Waisman, A, Notley, CA, Ehrenstein, MR, Kosco-Vilbois, M & Toellner, K-M 2013, 'Germinal center B cells govern their own fate via antibody feedback', *The Journal of Experimental Medicine*, vol. 210, no. 3, pp. 457-64. https://doi.org/10.1084/jem.20120150

Published February 18, 2013

Germinal center B cells govern their own fate via antibody feedback

Yang Zhang,[1] Michael Meyer-Hermann,[3,4] Laura A. George,[1] Marc Thilo Figge,[5] Mahmood Khan,[1] Margaret Goodall,[1] Stephen P. Young,[1] Adam Reynolds,[2] Francesco Falciani,[2] Ari Waisman,[6] Clare A. Notley,[7] Michael R. Ehrenstein,[7] Marie Kosco-Vilbois,[8] and Kai-Michael Toellner[1]

[1]Medical Research Council Centre for Immune Regulation, School of Immunity and Infection; and [2]Centre for Systems Biology, School of Biosciences; University of Birmingham, Birmingham B15 2TT, England, UK
[3]Department of Systems Immunology, Helmholtz Centre for Infection Research and [4]Biocenter for Life Sciences, Technical University of Braunschweig, 38124 Braunschweig, Germany
[5]Applied Systems Biology Research Group, Leibniz Institute for Natural Product Research and Infection Biology–Hans Knöll Institute, Friedrich Schiller University of Jena, 07745 Jena, Germany
[6]Institute for Molecular Medicine, University Medical Center of the Johannes Gutenberg University of Mainz, 55131 Mainz, Germany
[7]Centre for Rheumatology, University College London, London WC1E 6JF, England, UK
[8]NovImmune SA, 1228 Geneva, Switzerland

Affinity maturation of B cells in germinal centers (GCs) is a process of evolution, involving random mutation of immunoglobulin genes followed by natural selection by T cells. Only B cells that have acquired antigen are able to interact with T cells. Antigen acquisition is dependent on the interaction of B cells with immune complexes inside GCs. It is not clear how efficient selection of B cells is maintained while their affinity matures. Here we show that the B cells' own secreted products, antibodies, regulate GC selection by limiting antigen access. By manipulating the GC response with monoclonal antibodies of defined affinities, we show that antibodies in GCs are in affinity-dependent equilibrium with antibodies produced outside and that restriction of antigen access influences B cell selection, seen as variations in apoptosis, plasma cell output, T cell interaction, and antibody affinity. Feedback through antibodies produced by GC-derived plasma cells can explain how GCs maintain an adequate directional selection pressure over a large range of affinities throughout the course of an immune response, accelerating the emergence of B cells of highest affinities. Furthermore, this mechanism may explain how spatially separated GCs communicate and how the GC reaction terminates.

CORRESPONDENCE
Kai-Michael Toellner:
K.M.Toellner@bham.ac.uk

Abbreviations used: AID, activation-induced cytidine deaminase; BCR, B cell receptor; CGG, chicken gamma globulin; FDC, follicular dendritic cell; GC, germinal center; IC, immune complex; NP, 4-hydroxy-nitrophenyl.

Efficient long-term protection from infection is mediated by high-affinity antibodies, which can be provoked by foreign structures that stimulate B cells and raise T cell help (Jacobson et al., 1974). The process is initiated by engaging the B cell receptor (BCR) of a few antigen-specific B cells from the vast repertoire created in the bone marrow by random variable region gene segment recombination. These activated B cells proliferate and within a few days differentiate into plasma cells producing low-avidity early protective antibody (MacLennan et al., 2003; Goodnow et al., 2010). As soon as the first specific antibody is produced, germinal centers (GCs) develop (Jacob et al., 1991a; Liu et al., 1991). In GCs, B cells undergo affinity maturation of their BCR genes over time and will differentiate into longer-lived plasma cells or emerge as memory lymphocytes. Affinity maturation of B cells is an example of Darwinian evolution, as it is comprised of repeated cycles (Kepler and Perelson, 1993) of reproduction (i.e., proliferation; Hanna, 1964) and variation of IgV region genes via hypermutation (Berek et al., 1991; Jacob et al., 1991b)

Y. Zhang and M. Meyer-Hermann contributed equally to this paper.

The Rockefeller University Press $30.00
J. Exp. Med. 2013 Vol. 210 No. 3 457-464
www.jem.org/cgi/doi/10.1084/jem.20120150

Published February 18, 2013

followed by selection (Liu et al., 1989). Although much of the mechanism has been elucidated for modifying Ig genes (Muramatsu et al., 2007; Ramiro et al., 2007), less is certain as to how selection of the best-fitting BCR variants occurs. T cell help, critical for GC B cell selection, is dependent on the amount of antigen presented by B cells (Meyer-Hermann et al., 2006; Allen et al., 2007; Victora et al., 2010). Antigen uptake as well as direct B cell activation depends on BCR affinity, but only over a relatively small affinity range (Fleire et al., 2006). Furthermore, it is not understood how a stringent directional selection pressure is maintained while the affinity of B cells keeps rising. Therefore, we asked whether selection in GCs is dependent on access to antigen limited through antibody masking. Affinity-dependent competition between BCRs and the products of B cells themselves could be highly efficient, as it would generate a selection pressure that is directly dependent on the affinity of plasma cells derived from GCs. A selection threshold dependent on GC output would be dynamic, producing adequate selection stringency depending on the highest-affinity GC throughout the course of the GC response (Fig. 1 a).

RESULTS AND DISCUSSION

To test the hypothesis that antibody feedback impacts the appearance of high-affinity B cell variants, a novel mathematical model of the GC reaction was developed that represents effects of soluble antibody with antibody concentration and affinity that is dependent on GC output. The model included masking of antigen by antibodies (using realistic on–off kinetics) and inhibition of uptake of antigen retained on follicular dendritic cells (FDCs), which impacts follicular T cell help (Meyer-Hermann et al., 2006). Both antibody feedback mechanisms, i.e., masking and retention, were made dependent on the affinity of antibodies produced by GC-derived plasma cells. With these parameters, the simulations revealed that antibody feedback accelerates affinity maturation (Fig. 1 b) and induces a timely end to the GC reaction (Fig. 1 c). To test these predictions, mice deficient in the secreted form of IgM ($\mu_s^{-/-}$ mice; Ehrenstein et al., 1998) were immunized with immune complex (IC) to induce B cell activation and IC localization into B cell follicles. These mice developed GCs and, as predicted in silico, 4-hydroxy-nitrophenyl (NP)–specific IgG was of significantly lower affinity during the early stages of the GC response (Fig. 1 d). As $\mu_s^{-/-}$ mice should still have antibody feedback through IgG, long-term development of GCs was followed in animals completely devoid of soluble Ig ($IgH^{\mu\gamma1}$ mice; Waisman et al., 2007). As predicted in silico, GC responses were longer lived in the complete absence of soluble antibody (Fig. 1 e).

The outcome of these experiments thus motivated us to test in vivo whether there is an affinity-dependent equilibrium of

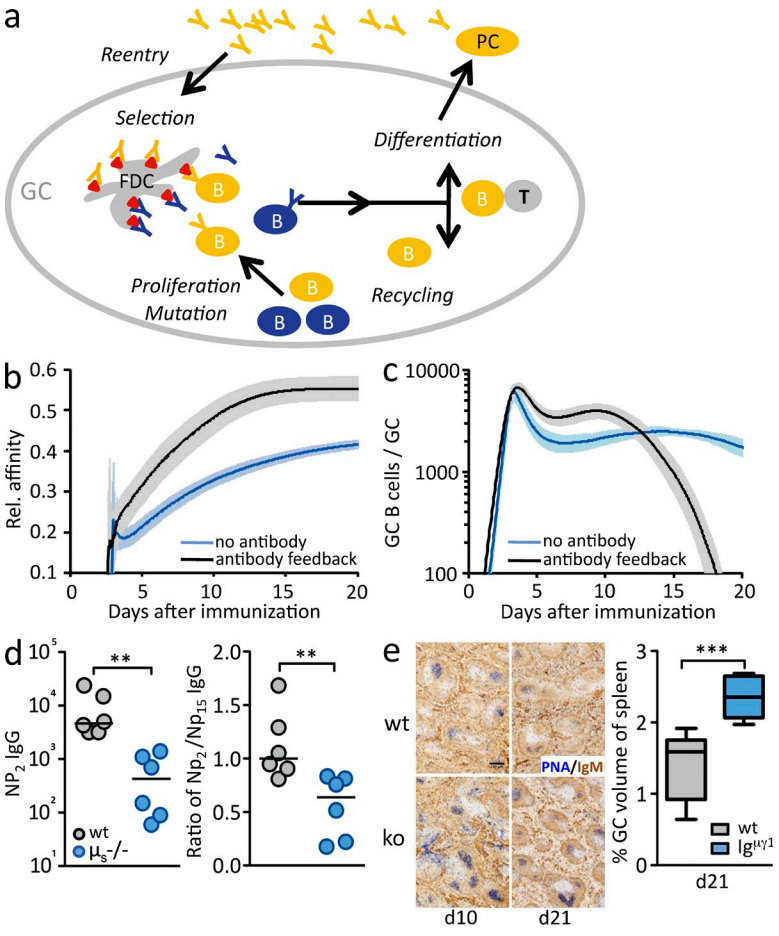

Figure 1. Effects of antibody on affinity maturation. (a) Antibody feedback hypothesis: B cells, after proliferating and hypermutating their Ig genes, interact with antigens deposited on FDCs. As these antigens are masked by early low-affinity antibodies (blue), only B cells with higher-affinity BCRs can effectively compete for access to antigen. Successful BCR engagement consequently allows interaction with T cells. Higher-affinity antibodies (yellow), produced by GC-derived plasma cells, reenter GCs and restrict antigen access over time. (b and c) In silico simulation of GC development predicts a more efficient increase in antibody affinity (b) and a clear termination of the GC reaction (c) with antibody feedback. (d) Amount of high-affinity NP-specific IgG and ratio of high-affinity/total antibody in blood 10 d after immunization of $\mu_s^{-/-}$ mice immunized with low-affinity IC of NP-CGG. Horizontal bars indicate median, and each symbol corresponds to one mouse. Data are from one experiment. (e) GC development in $IgH^{\mu\gamma1}$ mice. (left) Representative spleen images days 10 and 21 after immunization showing PNA for GCs and IgM for follicular areas. Bar, 100 µm. (right) GC volumes 21 d after immunization. Box plots indicate median, 50%, and 100% range. Data are from two independent experiments with a total of seven or eight mice per group. **, $P < 0.01$; ***, $P < 0.001$.

Published February 18, 2013

antibody inside and outside GCs. Primed C57BL/6 mice (allotype IgM^b) were immunized with ICs (IgM^a-IC) composed of NP coupled to chicken gamma globulin (CGG) and a nonmutated IgM^a antibody with low affinity to NP (clone Fab82, see Materials and methods). Exogenous IgM^a-IC localized in the marginal zone and B cell follicles within hours of administration and by 24 h deposited on the FDC networks (Fig. 2 a). Concomitantly, endogenous antibody was displaced from the FDC network (IgM^b in Fig. 2 [a and b]). 2 d after immunization, the time when the first NP-specific antibody–producing cells appear (Toellner et al., 1996), the injected antibody started to disappear and endogenous antibody reappeared on the FDC network (Fig. 2, a and b). 5 d after immunization, at the peak of the GC response, exogenous IgM^a antibody on FDCs was completely replaced by endogenous antibody (Fig. 2 a, bottom right).

To determine whether antibody replacement is dependent on the interaction between antibody and antigen, we used additional IgM^a monoclonal antibodies with affinities higher than clone Fab82. Two sets of IC with antibodies of lower intermediate (IntLow) and higher intermediate (IntHigh) affinities (Fig. 2 c) were created with NP-CGG and injected into primed IgM^b mice. In contrast to the low-affinity clone Fab82 (Fig. 2 a), both intermediate affinity antibodies were detectable in all mice in GCs 5 d after immunization (Fig. 2, d and e). Furthermore, significantly more antibodies were present in GCs of mice that had received the higher-affinity variant (IntHigh; Fig. 2, e [left] and f). Yet the total amount of NP-specific antibody on FDCs was similar whatever antibody had been injected (Fig. 2, d and e, right). These results demonstrate, for the first time, a dynamic process of antibody turnover within GC-localized IC and indicate that the replacement of antibody is affinity dependent.

To test whether antibody produced by plasma cells outside GCs can enter and affect B cell selection in established

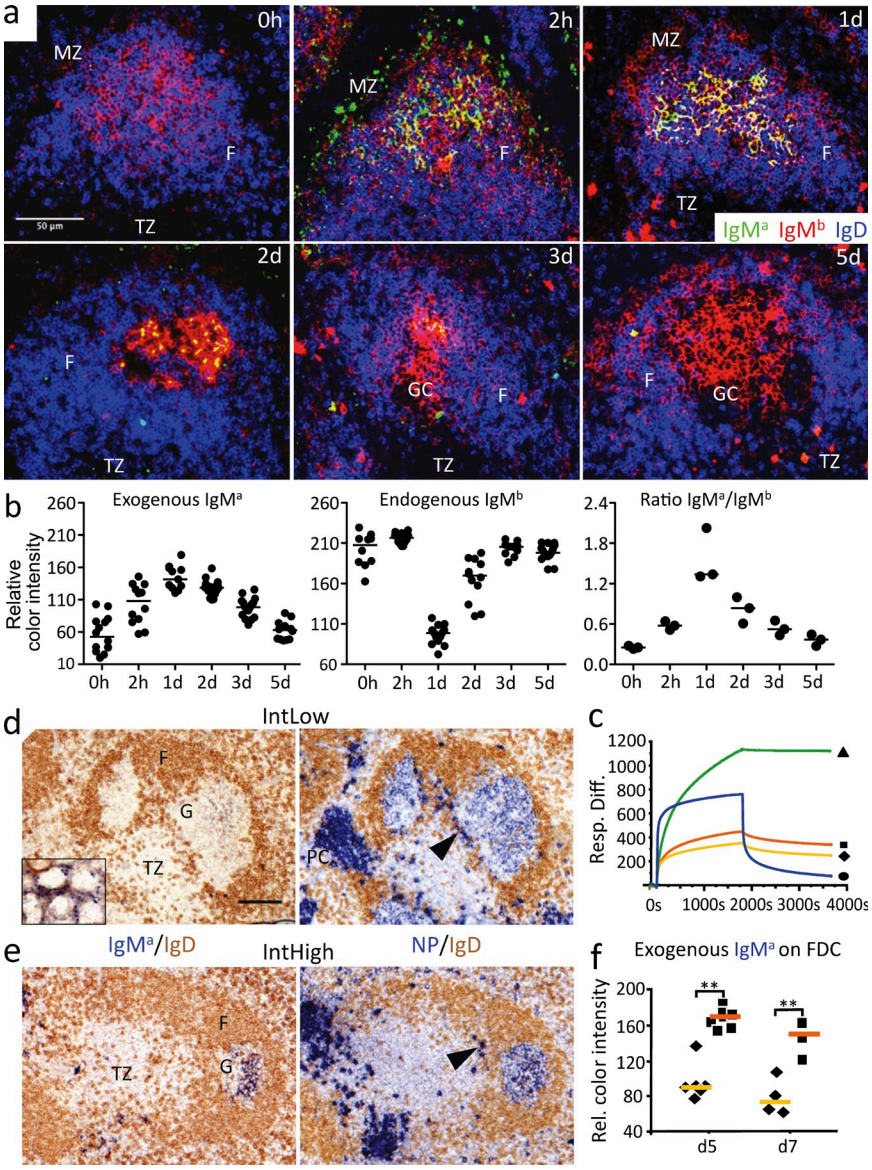

Figure 2. Affinity-dependent equilibrium of antibody inside and outside GCs. (a) Representative images of splenic B cell follicles from a time course after i.v. injection of low-affinity IgM^a-IC. IgM^a, endogenous IgM^b, and IgD to show follicles (F) were used. MZ, marginal zone; TZ, T zone. (b) Quantification of the staining intensity for IgM^a and IgM^b from a similar series of immunoenzymatically stained tissues shows appearance and replacement of the injected antibody. (left and middle) Each symbol represents one FDC network area in different GCs. (right) Mean ratio of IgM^a/IgM^b staining intensities with each symbol representing one animal. (c) Surface plasmon resonance from the four different NP-specific IgM^a monoclonal antibodies produced for this study. Based on the association and dissociation kinetics, antibody affinity was ranked as Low (clone Fab82; blue ●) < IntLow (clone 2.315; yellow ◆) < IntHigh (clone 1.198; orange ■) < High (clone 1.197; green ▲). The same labels are used throughout this manuscript. (d, left) IntLow-affinity IgM^a 5 d after IgM^a-IC immunization. Inset shows same staining at higher magnification. (right) Total NP-specific antibody showing B cells and IC in GCs, plasma cells in red pulp, and plasmablasts in GC vicinity (arrowhead). (e, left) IntHigh-affinity IgM^a 5 d after immunization. (right) Total NP-specific antibody. The arrowhead indicates GC-associated plasmablasts. G, GC; PC, plasma cell. Bars, 50 µm. (f) Semiquantitative analysis of IgM^a density on FDC networks. Each symbol corresponds to the median IgM^a density on FDC networks in one animal. Data are representative of three independent experiments. Horizontal bars indicate median. **, $P < 0.01$.

Published February 18, 2013

JEM

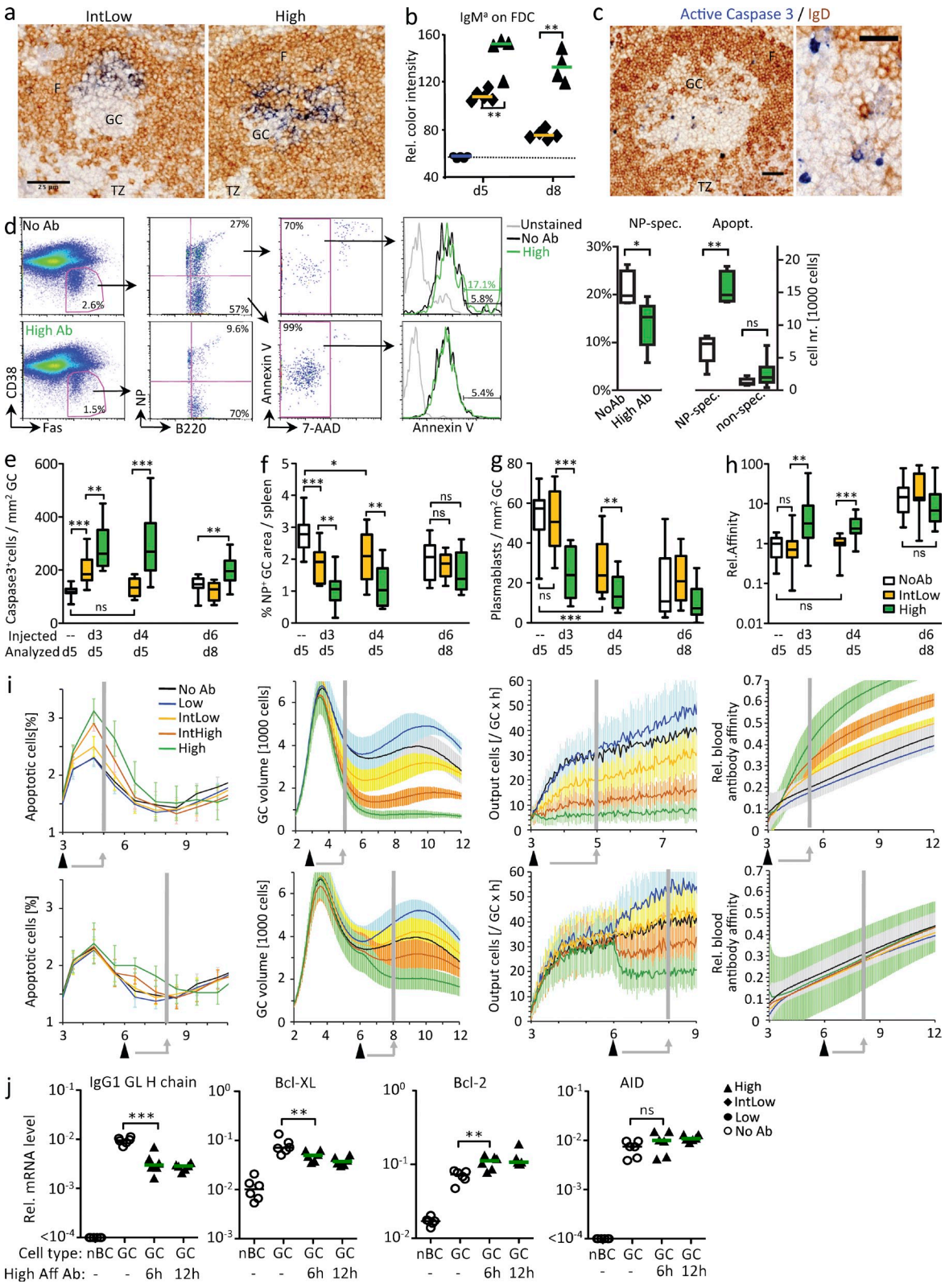

Figure 3. Effects of antibody injection on established GCs. (a) IgMa (blue) injected 3 d after immunization with NP-CGG was analyzed 48 h later. IgD is brown. F, follicle; TZ, T zone. (b) Quantitation of IgMa levels on FDC networks for IgMa injected 3 or 6 d after NP-CGG immunization, analyzed 2 d later (dotted line: background staining level). (c) Apoptotic B cells as indicated by active form of caspase 3. Bars, 25 µm. (d) Numbers of NP-binding GC B cells and NP-specific GC B cells staining for Annexin V 24 h after injection of NP-specific high-affinity antibody. (left) Representative FACS plot showing gating

Published February 18, 2013

GCs, the IgM[a] antibodies of either Low, IntLow, or highest (High) affinities were injected either 3 d (just after GCs had formed) or 6 d (when GC B cells had 3 d to mature to higher affinity) after immunization with soluble NP-CGG. The tissues were assessed 2 d later, i.e., day 5 or 8 (Fig. 3, a and b). 2 d after injection, Low-affinity antibody could not be detected on the FDC network of GCs, whereas both the IntLow- and High-affinity antibodies could be observed in the GCs (Fig. 3 a). The amount of antibody found correlated with the affinity of the antibody (Fig. 3 b). Importantly, maturation of the immune response affected antibody entry, as IntLow antibody was not able to enter mature GCs in substantial amounts after higher-affinity endogenous antibodies had been produced (Fig. 3 b, d8). Analyzing GC B cell differentiation revealed that when antibodies entered GCs, B cell selection was affected. Assessment of the active form of caspase-3 (Fig. 3 c) and Annexin V staining (Fig. 3 d) demonstrated increased apoptosis in NP-specific GC B cells. The amount of apoptosis correlated with the affinity of the injected antibody (Fig. 3 e). Injection of the IntLow-affinity antibody at early stages had less effect than High-affinity antibody, and it had no effect in mature GCs, supporting the hypothesis that antibody entering GCs competes with GC B cells in an affinity-dependent way. Increased apoptosis substantially reduced GC volumes (Fig. 3, a and f). Also, output from GCs was reduced with fewer plasmablasts present in the GC periphery (Fig. 3 g). Surprisingly, administration of the antibody variants even affected the affinity of endogenous antigen-specific IgG in blood. High-affinity antibody drove the response quicker to higher-affinity IgG (Fig. 3 h), but only when it was given at an early stage. Collectively, these observations demonstrate an increase in B cell selection stringency dependent on the affinity of antibody present inside GC.

We next asked whether these in vivo effects of antibody can be explained by competition for antigen using our new mathematical model. In silico experiments showed that constraining antigen access and uptake by the GC B cells are both necessary and sufficient to replicate the complex in vivo effects of antibody on B cell survival, GC volume, plasma cell output, and affinity (Fig. 3 i), supporting the conclusion that antibody feedback is the mechanism responsible for the effects of antibody observed in vivo. Affinity-dependent variation in antigen uptake is an important factor because it determines the fitness of B cells to interact with T cells in silico (not depicted). To test in vivo whether competition from High-affinity antibody leads to reduced B cell–T cell interaction, we analyzed IgG1 heavy chain germline transcription, which is a good indicator of T-dependent B cell activation (Toellner et al., 1996). Indeed, within 6 h, injection of High-affinity antibody led to reduced production of IgG1 heavy chain germline transcripts (Fig. 3 j). This confirms that antibody-dependent restriction of antigen access and uptake inhibits downstream T cell–B cell interaction, ultimately leading to death by neglect (Fig. 3 j). Upstream processes such as expression of activation-induced cytidine deaminase (AID), essential for hypermutation, were not influenced (Fig. 3 j).

Several mechanisms for the preferential selection of affinity-matured GC B cells have been proposed. T cells in GCs help the B cells that have been most efficient in taking up and presenting antigen (Meyer-Hermann et al., 2006; Allen et al., 2007; Victora et al., 2010). Although BCR ligation has been shown to induce B cell activation and antigen presentation to T cells in an affinity-dependent way, this affinity dependence acts only over a relatively small affinity range (Fleire et al., 2006). As GC B cell affinity evolves, one would expect a mechanism that raises the selection pressure in line with the evolution of B cell clones (Tarlinton and Smith, 2000). During infections, large amounts of antigen are produced over a prolonged time. Therefore, direct competition of B cells for antigen or consumption of antigen is an unlikely mechanism to keep stringent selection pressure over a prolonged response. We show here that, dependent on its affinity, secreted antibody enters GCs and, over time, limits antigen access. As GC B cell affinity evolves, the selection pressure rises, gradually restricting access to and uptake of antigen. This may complement direct affinity-dependent B cell activation (Fleire et al., 2006) and lead to efficient directional selection of B cells over a large affinity range. Indeed, mice deficient in soluble IgM have delayed affinity maturation (Boes et al., 1998; Ehrenstein et al., 1998). This study focused on the analysis of effects of IgM antibodies on affinity maturation. Ig class switching may provide another layer of regulation, reducing antibody avidity once the response has advanced and providing a range of additional signals through the Ig heavy chain (Song et al., 1998; Hjelm et al., 2006).

One of the conundrums of GC biology has been whether responses in different GCs interact. Entry and exit of B cells from GCs have been observed, but these are typically naive B cells (Hauser et al., 2007; Schwickert et al., 2007), and different GCs usually show separate genealogies (Jacob and Kelsoe, 1992). The antibody-dependent selection mechanism demonstrated here makes inter-GC B cell migration dispensable,

scheme. (right) Quantitative data from two independent experiments with a total of nine mice per group. (e) Density of apoptotic cells at different intervals after injection of antibody affinity in early stage (day 5) or later stage (day 8) GCs. (f) NP-specific GC sizes. (g) NP-specific GC-associated plasmablast output (Fig. 2, d and e, arrowheads). (h) NP_2/NP_{15} binding ratio of NP-specific IgG in blood, expressed relative to median level of the day 5 control. Each symbol corresponds to one animal. Data are representative of three independent experiments. Horizontal bars show medians color coded as in i. Boxes are 50% range, and whiskers are 100% range. (i) In silico effect of antibodies of different affinities. Arrowheads indicate in silico antibody injection 3 (continuous lines) or 6 d (broken lines) after immunization. Vertical gray lines correspond to the time of analysis of the in vivo experiments. Data show means and standard deviation of 20 in silico experiments. (j) Change in IgG1 heavy chain germline RNA, Bcl-Xl, and Bcl2, but no significant change in AID expression in FACS-sorted GC B cells 6 or 12 h after antibody injection. Symbols for No Ab, IntLow, and High-affinity antibody groups correspond to individual animals. Data are representative of two independent experiments. Horizontal bars indicate median. nBC, naive B cells. *, $P < 0.05$; **, $P < 0.01$; ***, $P < 0.001$.

Published February 18, 2013

as soluble antibody produces a systemic selection threshold. At some stage it can be expected that the restriction of antigen access is too strong to allow for B cell survival, ending the GC reaction. Indeed, in silico experiments predict a natural end to the GC reaction once antibody affinity is sufficiently high (Fig. 1, b and c), and mice without antibody feedback have prolonged GC responses (Fig. 1 d).

Artificially adding exogenous antibody of moderate avidity may be a way to manipulate vaccine responses. In silico modeling indicates that antibodies of low affinity added at the start of a reaction will accelerate the early stages of affinity maturation, and preliminary experiments using IgM in vivo show that this strategy may be effective.

Antibody feedback with a dynamic selection threshold accelerates optimization of Ig variable region genes during the development of an antibody response. Changes in selection pressure caused by consumption of limited resources or ecological changes induced by evolving species have been described as factors shaping evolution (Schoener, 2011). In the case of the GC, B cells produce their own selective environment, bootstrapping themselves by producing a mediator that tunes their own selection and provides adequate selection pressure throughout the entire environment. This maximizes the speed of evolution of B cell clones systemically, which surely is an evolutionary adaptation to the enormous selection pressure caused by our continuous fight to adapt to new pathogens.

MATERIALS AND METHODS

Mice and immunizations. Specified pathogen–free C57BL/6J mice were primed with 50 µg alum–precipitated CGG mixed with 10^7 heat-killed *Bordetella pertussis* and challenged i.v. with 20 µg NP_{18}-CGG–soluble or complexed for 1 h with 180 µg NP-specific IgM^a. NP-specific IgM^a was injected i.v. at 90 µg/200 µl saline.

Unprimed soluble IgM-deficient $\mu_s^{-/-}$ mice (Ehrenstein et al., 1998) and soluble Ig-deficient $IgH^{\mu\gamma 1}$ mice (Waisman et al., 2007) were immunized i.p. with NP-CGG complexed with low-affinity NP-specific antibody. All procedures on mice were covered by a project license approved by the UK Home Office.

NP-specific IgM^a antibodies. Mice with targeted insertions for NP-specific V-regions of different affinities, QM (Cascalho et al., 1996), B1-8 (gift from M. Reth, Max Planck Institut, Freiburg, Germany; Sonoda et al., 1997), and B1-8^{high} (M.C. Nussenzweig, The Rockefeller University, New York, NY; Shih et al., 2002), were immunized i.p. with NP-Ficoll 4 d before removing the spleens. Splenocytes were fused with NS0 plasmacytoma cells and selected in HAT (hypoxanthine-aminopterin-thymidine) medium. Supernatants from viable clones were screened for NP-specific antibody production and Ig class using ELISA plates coated with NP-BSA. Hybridomas were expanded and grown in hollow fiber bioreactors, and the antibody was purified by affinity chromatography using NP-Sepharose and dialyzed against PBS, pH 7.4. Antibody-binding kinetics were determined by plasmon surface resonance in a Biacore 3000 (GE Healthcare) using NP_{15}-BSA–coupled chips. 125 nM antibody in PBS, pH 7.4 (38°C), was flown at a flow rate of 5 µl/min for 30 min. This was followed by dissociation at 38°C with PBS. Low affinity (clone Fab82) was gift from F. Gaspal (University of Birmingham, Birmingham, England, UK).

Immunohistology. Spleen sections were prepared and double-stained as described previously (Marshall et al., 2011). The following additional antibodies were used: IgM^a FITC (DS-1; BD), IgM^b biotin (AF6-78; BD), rabbit anti–mouse active caspase 3 (C92-605; BD), and biotinylated peanut agglutinin (PNA; Vector Laboratories). FITC was detected with a secondary rabbit anti-FITC antiserum (Dako), followed by biotinylated swine anti–rabbit antiserum (Dako) and StreptABComplex/AP as described previously (Marshall et al., 2011). In the final step, color was developed using FastBlue and DAB (3,3′-diaminobenzidine; Sigma-Aldrich). A semiquantitative measurement of the appearance and disappearance of IgM^a-IC in GCs was performed using ImageJ (National Institutes of Health). Spleen sections were stained for IgM^a or IgM^b using FastBlue plus IgD using DAB. To quantify FastBlue precipitate, blue and brown staining were separated using the color deconvolution plugin with inbuilt vectors for FastBlue and DAB. Regions of interest were drawn around areas representing ICs on the FDC network, and mean pixel intensity was determined. Median intensities of IgM^a and IgM^b staining were quantified from several spleen sections. The method was validated by comparing with staining intensities of parallel sections stained with FITC-labeled antibodies.

For fluorescence staining, biotinylated IgM^b was incubated by Cy3-Streptavidin (Stratech). IgM^a FITC and IgD Alexa Fluor 647 (eBioscience) were used. The slides were mounted in Prolong Gold antifade mounting medium (Invitrogen). Images were taken on a DM6000 fluorescent microscope (Leica).

ELISA. Serial dilutions of serum samples were analyzed by ELISA on NP_{15}-BSA–coupled microtiter plates to detect NP-specific antibody. NP_2-BSA–coupled microtiter plates were used to measure the high-affinity antibody fraction. Relative affinity was calculated by dividing relative antibody concentration from NP_2-BSA–coupled plates by concentration derived from NP_{15}-coupled plates.

Gene expression in GC cells. Splenic B cells of B1-8 mice (Sonoda et al., 1997) that are Igk deficient (Zou et al., 1993) and express eYFP (gift from J. Caamaño, University of Birmingham; Srinivas et al., 2001) were prepared in RPMI1640 medium containing 5% FCS and 10 mM EDTA (Sigma-Aldrich) using CD43-labeled magnetic microbeads (Miltenyi Biotech). 10^5 B cells were injected i.v. into CGG-primed C57BL/6 mice. Hosts were immunized 24 h later with NP-CGG i.p. 4 d after challenge, 90 µg of High-affinity IgM^a (clone 1.197) was injected i.v., and 6 h later, splenocytes were stained using Hoechst 33258, B220 PE-Cy5, Fas PE-Cy7, CD138 APC (BD), and NP-PE. GC B cells were sorted as $B220^{high}$, $eYFP^+$, NP^+, Fas^{high}, $CD138^-$ in a high-speed cells sorter (MoFlo; Beckman Coulter). Real-time RT-PCR for IgG1 germline heavy chain and AID was performed in multiplex with β2-microglobulin–specific primers and probes as described previously (Marshall et al., 2011); other primers and probes were from Applied Biosystems.

Flow cytometry. Splenocytes were stained with B220 FITC, Fas PE-Cy7, CD38 Pacific Blue (BD), and NP-PE. Cy5 Annexin V apoptosis detection kit (BD) was used for staining apoptotic and dead cells. Apoptotic GC B cells were gated as $B220^+$, NP-binding or nonbinding, $CD38^-$, Fas^+, Annexin V^+, 7-AAD^- (Fig. 3 d).

Statistical analysis. All statistical analysis was performed using nonparametric one-sided Wilcoxon Mann-Whitney U Test. Statistics throughout were performed by comparing data obtained from all independent experiments. P-values are indicated throughout with * for $P < 0.05$, ** for $P < 0.01$, and *** for $P < 0.001$.

In silico GC model. The GC model (Figge et al., 2008) was extended to represent soluble antibodies and to describe the dynamics of free antigen present on FDCs with the potential to interact with BCRs on B cells: It was assumed that GC-derived plasma cells start producing antibodies 1 d after induction of plasma cell differentiation. The produced antibodies spread systemically, such that the antibodies found in the modeled specific GC stem from a mixture of all GCs in the organism. Antibodies were classified in 11 affinity bins B_i, with $i = 0,\ldots,10$, and produced by plasma cells Q_i according to $dQ_i/dt = r_{PMdiff} \cdot P_i$, where P_i is the number of plasma cells outside the GC

and $r_{PMdiff} = \ln(2)/h$ is the rate of differentiation of GC-derived plasma cells P_i to Q_i. The P_i are generated according to $dP_i/dt = P_{i,GC}(t) - r_{PMdiff} P_i$, with $P_{i,GC}(t)$ the number of plasma cells exiting the modeled GC at time t. The antibody flora in each GC is then derived from the extrapolated antibody-producing plasma cells in the whole organism by $dB_i/dt = (N_{GC}\, r_{PM}/V_{blood})\, P_i - gB_i$ using $r_{PM} = 2 \times 10^{-18}$ mol/h per cell (Randall et al., 1992), $g = \ln(2)/(10\ d)$, $N_{GC} = 100$, and $V_{blood} = 4$ ml. This gives rise to a concentration of antibodies B_i in mol/l.

Although the amount of antibodies was considered a global GC property, the amount of free antigen, $A(x)$, is a local property of the FDCs. Thus, at every FDC node, we solved the chemical kinetics of IC formation by $dC_i(x)/dt = k_{on}A(x)B_i - k_{i,off}C_i(x)$. The on-rate k_{on} was assumed constant, whereas the off-rate $k_{i,off} = k_{on}/10^{5.5+0.4i}$ reflected the variation of the antibody affinity to the antigen in the different bins i over a range of 4 orders of magnitude. We used $k_{on} = 10^6$/(mol s; Batista and Neuberger, 1998); on the spatial lattice for cell migration and interaction, every FDC node was associated with a dynamic amount of available free antigen depending on the amount of already produced antibodies and their distribution on the affinity bins.

B cells locally compete with the soluble antibodies for binding of free antigen. Without competition, the binding probability (or affinity) is assumed to depend on the Hamming distance d to the optimal clone in number of mutations in a four-dimensional shape space according to a Gaussian $a = \exp(-d^2/w^2)$ between 0 and 1 using a width of $w = w_0(1 - A)$, with $w_0 = 2.8$ mutation (Figge et al., 2008) and A being the average affinity of all produced (or injected) antibodies with affinities a calculated with the same Gaussian in the noncompetition limit, i.e., with width $w = w_0$. This model reflects antigen masking plus competitive binding of the remaining free antigen retained by higher-affinity antibodies.

This study was supported by the European Union within the New and Emerging Science and Technology project MAMOCELL, the Medical Research Council, and the Wellcome Trust. M. Meyer-Hermann was supported by the BMBF (Bundesministerium für Bildung und Forschung) GerontoSys initiative and the Human Frontier Science Programme.

The authors have no competing financial interests.

Submitted: 26 April 2012
Accepted: 16 January 2013

REFERENCES

Allen, C.D., T. Okada, and J.G. Cyster. 2007. Germinal-center organization and cellular dynamics. *Immunity*. 27:190–202. http://dx.doi.org/10.1016/j.immuni.2007.07.009

Batista, F.D., and M.S. Neuberger. 1998. Affinity dependence of the B cell response to antigen: a threshold, a ceiling, and the importance of off-rate. *Immunity*. 8:751–759. http://dx.doi.org/10.1016/S1074-7613(00)80580-4

Berek, C., A. Berger, and M. Apel. 1991. Maturation of the immune response in germinal centers. *Cell*. 67:1121–1129. http://dx.doi.org/10.1016/0092-8674(91)90289-B

Boes, M., C. Esau, M.B. Fischer, T. Schmidt, M. Carroll, and J. Chen. 1998. Enhanced B-1 cell development, but impaired IgG antibody responses in mice deficient in secreted IgM. *J. Immunol.* 160:4776–4787.

Cascalho, M., A. Ma, S. Lee, L. Masat, and M. Wabl. 1996. A quasi-monoclonal mouse. *Science*. 272:1649–1652. http://dx.doi.org/10.1126/science.272.5268.1649

Ehrenstein, M.R., T.L. O'Keefe, S.L. Davies, and M.S. Neuberger. 1998. Targeted gene disruption reveals a role for natural secretory IgM in the maturation of the primary immune response. *Proc. Natl. Acad. Sci. USA*. 95:10089–10093. http://dx.doi.org/10.1073/pnas.95.17.10089

Figge, M.T., A. Garin, M. Gunzer, M. Kosco-Vilbois, K.M. Toellner, and M. Meyer-Hermann. 2008. Deriving a germinal center lymphocyte migration model from two-photon data. *J. Exp. Med.* 205:3019–3029. http://dx.doi.org/10.1084/jem.20081160

Fleire, S.J., J.P. Goldman, Y.R. Carrasco, M. Weber, D. Bray, and F.D. Batista. 2006. B cell ligand discrimination through a spreading and contraction response. *Science*. 312:738–741. http://dx.doi.org/10.1126/science.1123940

Goodnow, C.C., C.G. Vinuesa, K.L. Randall, F. Mackay, and R. Brink. 2010. Control systems and decision making for antibody production. *Nat. Immunol.* 11:681–688. http://dx.doi.org/10.1038/ni.1900

Hanna, M.G. Jr. 1964. An Autoradiographic Study of the Germinal Center in Spleen White Pulp During Early Intervals of the Immune Response. *Lab. Invest.* 13:95–104.

Hauser, A.E., T. Junt, T.R. Mempel, M.W. Sneddon, S.H. Kleinstein, S.E. Henrickson, U.H. von Andrian, M.J. Shlomchik, and A.M. Haberman. 2007. Definition of germinal-center B cell migration in vivo reveals predominant intrazonal circulation patterns. *Immunity*. 26:655–667. http://dx.doi.org/10.1016/j.immuni.2007.04.008

Hjelm, F., F. Carlsson, A. Getahun, and B. Heyman. 2006. Antibody-mediated regulation of the immune response. *Scand. J. Immunol.* 64:177–184. http://dx.doi.org/10.1111/j.1365-3083.2006.01818.x

Jacob, J., and G. Kelsoe. 1992. In situ studies of the primary immune response to (4-hydroxy-3-nitrophenyl)acetyl. II. A common clonal origin for periarteriolar lymphoid sheath-associated foci and germinal centers. *J. Exp. Med.* 176:679–687. http://dx.doi.org/10.1084/jem.176.3.679

Jacob, J., R. Kassir, and G. Kelsoe. 1991a. In situ studies of the primary immune response to (4-hydroxy-3-nitrophenyl)acetyl. I. The architecture and dynamics of responding cell populations. *J. Exp. Med.* 173:1165–1175. http://dx.doi.org/10.1084/jem.173.5.1165

Jacob, J., G. Kelsoe, K. Rajewsky, and U. Weiss. 1991b. Intraclonal generation of antibody mutants in germinal centres. *Nature*. 354:389–392. http://dx.doi.org/10.1038/354389a0

Jacobson, E.B., L.H. Caporale, and G.J. Thorbecke. 1974. Effect of thymus cell injections on germinal center formation in lymphoid tissues of nude (thymusless) mice. *Cell. Immunol.* 13:416–430. http://dx.doi.org/10.1016/0008-8749(74)90261-5

Kepler, T.B., and A.S. Perelson. 1993. Cyclic re-entry of germinal center B cells and the efficiency of affinity maturation. *Immunol. Today*. 14:412–415. http://dx.doi.org/10.1016/0167-5699(93)90145-B

Liu, Y.J., D.E. Joshua, G.T. Williams, C.A. Smith, J. Gordon, and I.C. MacLennan. 1989. Mechanism of antigen-driven selection in germinal centres. *Nature*. 342:929–931. http://dx.doi.org/10.1038/342929a0

Liu, Y.J., J. Zhang, P.J. Lane, E.Y. Chan, and I.C. MacLennan. 1991. Sites of specific B cell activation in primary and secondary responses to T cell-dependent and T cell-independent antigens. *Eur. J. Immunol.* 21:2951–2962. http://dx.doi.org/10.1002/eji.1830211209

MacLennan, I.C., K.-M. Toellner, A.F. Cunningham, K. Serre, D.M. Sze, E. Zúñiga, M.C. Cook, and C.G. Vinuesa. 2003. Extrafollicular antibody responses. *Immunol. Rev.* 194:8–18. http://dx.doi.org/10.1034/j.1600-065X.2003.00058.x

Marshall, J.L., Y. Zhang, L. Pallan, M.C. Hsu, M. Khan, A.F. Cunningham, I.C. MacLennan, and K.M. Toellner. 2011. Early B blasts acquire a capacity for Ig class switch recombination that is lost as they become plasmablasts. *Eur. J. Immunol.* 41:3506–3512. http://dx.doi.org/10.1002/eji.201141762

Meyer-Hermann, M.E., P.K. Maini, and D. Iber. 2006. An analysis of B cell selection mechanisms in germinal centers. *Math. Med. Biol.* 23:255–277. http://dx.doi.org/10.1093/imammb/dql012

Muramatsu, M., H. Nagaoka, R. Shinkura, N.A. Begum, and T. Honjo. 2007. Discovery of activation-induced cytidine deaminase, the engraver of antibody memory. *Adv. Immunol.* 94:1–36. http://dx.doi.org/10.1016/S0065-2776(06)94001-2

Ramiro, A., B. Reina San-Martin, K. McBride, M. Jankovic, V. Barreto, A. Nussenzweig, and M.C. Nussenzweig. 2007. The role of activation-induced deaminase in antibody diversification and chromosome translocations. *Adv. Immunol.* 94:75–107. http://dx.doi.org/10.1016/S0065-2776(06)94003-6

Randall, T.D., R.M. Parkhouse, and R.B. Corley. 1992. J chain synthesis and secretion of hexameric IgM is differentially regulated by lipopolysaccharide and interleukin 5. *Proc. Natl. Acad. Sci. USA*. 89:962–966. http://dx.doi.org/10.1073/pnas.89.3.962

Schoener, T.W. 2011. The newest synthesis: understanding the interplay of evolutionary and ecological dynamics. *Science*. 331:426–429. http://dx.doi.org/10.1126/science.1193954

Schwickert, T.A., R.L. Lindquist, G. Shakhar, G. Livshits, D. Skokos, M.H. Kosco-Vilbois, M.L. Dustin, and M.C. Nussenzweig. 2007. In vivo imaging of germinal centres reveals a dynamic open structure. *Nature*. 446:83–87. http://dx.doi.org/10.1038/nature05573

Shih, T.A., M. Roederer, and M.C. Nussenzweig. 2002. Role of antigen receptor affinity in T cell-independent antibody responses in vivo. *Nat. Immunol.* 3:399–406. http://dx.doi.org/10.1038/ni776

Song, H., X. Nie, S. Basu, and J. Cerny. 1998. Antibody feedback and somatic mutation in B cells: regulation of mutation by immune complexes with IgG antibody. *Immunol. Rev.* 162:211–218. http://dx.doi.org/10.1111/j.1600-065X.1998.tb01443.x

Sonoda, E., Y. Pewzner-Jung, S. Schwers, S. Taki, S. Jung, D. Eilat, and K. Rajewsky. 1997. B cell development under the condition of allelic inclusion. *Immunity*. 6:225–233. http://dx.doi.org/10.1016/S1074-7613(00)80325-8

Srinivas, S., T. Watanabe, C.S. Lin, C.M. William, Y. Tanabe, T.M. Jessell, and F. Costantini. 2001. Cre reporter strains produced by targeted insertion of EYFP and ECFP into the ROSA26 locus. *BMC Dev. Biol.* 1:4. http://dx.doi.org/10.1186/1471-213X-1-4

Tarlinton, D.M., and K.G. Smith. 2000. Dissecting affinity maturation: a model explaining selection of antibody-forming cells and memory B cells in the germinal centre. *Immunol. Today*. 21:436–441. http://dx.doi.org/10.1016/S0167-5699(00)01687-X

Toellner, K.-M., A. Gulbranson-Judge, D.R. Taylor, D.M.-Y. Sze, and I.C.M. MacLennan. 1996. Immunoglobulin switch transcript production in vivo related to the site and time of antigen-specific B cell activation. *J. Exp. Med.* 183:2303–2312. http://dx.doi.org/10.1084/jem.183.5.2303

Victora, G.D., T.A. Schwickert, D.R. Fooksman, A.O. Kamphorst, M. Meyer-Hermann, M.L. Dustin, and M.C. Nussenzweig. 2010. Germinal center dynamics revealed by multiphoton microscopy with a photoactivatable fluorescent reporter. *Cell*. 143:592–605. http://dx.doi.org/10.1016/j.cell.2010.10.032

Waisman, A., M. Kraus, J. Seagal, S. Ghosh, D. Melamed, J. Song, Y. Sasaki, S. Classen, C. Lutz, F. Brombacher, et al. 2007. IgG1 B cell receptor signaling is inhibited by CD22 and promotes the development of B cells whose survival is less dependent on Igα/β. *J. Exp. Med.* 204:747–758. http://dx.doi.org/10.1084/jem.20062024

Zou, Y.R., S. Takeda, and K. Rajewsky. 1993. Gene targeting in the Ig kappa locus: efficient generation of lambda chain-expressing B cells, independent of gene rearrangements in Ig kappa. *EMBO J.* 12:811–820.